ACS APPLIED MATERIALS & INTERFACES

Research Article

www.acsami.org

Phase-Controlled Synthesis of Cobalt Sulfides for Lithium Ion Batteries

Yaoming Wang,[†] Jianjun Wu,[†] Yufeng Tang,[†] Xujie Lü,*[,†] Chongyin Yang,[†] Mingsheng Qin,[†] Fuqiang Huang,*[,†,‡] Xin Li,[†,§] and Xia Zhang*[,§]

[†]CAS Key Laboratory of Materials for Energy Conversion, Shanghai Institute of Ceramics, Chinese Academy of Sciences, Shanghai 200050, P.R. China

[‡]Beijing National Laboratory for Molecular Sciences and State Key Laboratory of Rare Earth Materials Chemistry and Applications, College of Chemistry and Molecular Engineering, Peking University, Beijing 100871, P.R. China

[§]College of Science, Northeastern University, Shenyang 110004, P.R.China

Supporting Information

ABSTRACT: The polyhedral CoS_2 with a narrow size distribution was synthesized by a facile solid-state assembly process in a sealed silica tube. The flux of potassium halide (KX; X = Cl, Br, I) plays a crucial role in the formation of polyhedrons and the size distribution. The S_2^{2-} groups in CoS_2 can be controllably withdrawn during heat treatment in air. The obtained phases and microstructures of CoS_2, Co_3S_4, CoS, Co_9S_8, and CoO depended on heating temperature and time. These cobalt materials, successfully used as the electrodes of lithium ion batteries, possessed good cycling stability in lithium ion batteries. The discharge capacities of 929.1 and 835.2 mAh g^{-1} were obtained for CoS_2 and CoS respectively, and 76% and 71% of the capacities remained after 10 cycles. High capacities and good cycle performance make them promising candidates for lithium ion batteries. The approach combining solid-state assembly and heat treatment provides a simple and versatile way to prepare various metal chalcogeides for energy storage applications.

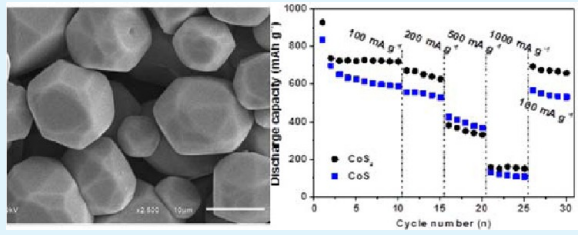

KEYWORDS: *cobalt sulfides, solid-state assembly, polyhedrons, electrode materials, lithium ion batteries, cycling stability*

1. INTRODUCTION

Cobalt sulfides (CoS_x) with different stoichiometric compositions such as CoS_2, Co_3S_4, CoS, and Co_9S_8 have attracted great attention due to their unique physical and chemical properties. The phases of CoS_x used in catalysis,[1] lithium ion batteries,[2−5] alkaline secondary batteries,[6] and magnetic materials[7−9] have been wildly investigated. Lithium ion batteries play an extremely important role in the fast-developing field of new energy. Since commercial carbonaceous anode materials are insufficient,[10] cobalt sulfides are promising anode materials due to their high electrical conductivity, good thermal stability, and high theoretical capacity.[11,12] As reported by Poizot et al., the reaction mechanism of sulfides with Li^+ can be described below:[13]

$$M^{n+}(X) + ne^- + nLi^+ \Leftrightarrow M^0 + nLi(X) \quad (X = S, O) \tag{1}$$

Many approaches have been explored to synthesize metal sulfides, including solid-state reaction,[2,14] a hydrothermal/solvothermal method,[4,5,15] an arc-discharge method,[16] a catalyzed transport method,[17] and chemical vapor decomposition.[18] Among those methods, the solid-state reaction is widely used in industry and easily operated. However, a prolonged reaction time is required to obtain the product in the reaction of metals and sulfur, for example, 120 h for the preparation of CoS_2.[2] Therefore, it is highly desirable to develop a rapid and cost-effective approach for the mass production of cobalt sulfides.

In this study, polyhedral cobalt sulfides (e.g., CoS_2) with a uniform size distribution were prepared via a potassium halide assisted solid-state assembly (SSA) process in 9 h at 850 °C. The reaction parameters such as the flux of potassium halides and post-heat treatment (temperature, time) were investigated in detail. Other cobalt chalcogenides (e.g., $CoSe_2$, CoSSe) were synthesized by the same method. The as-prepared cobalt sulfides were successfully applied as the electrode materials in lithium ion batteries and possessed high capacity and excellent stability. Thus, these materials have become electrode candidates for rechargeable lithium ion batteries.

2. EXPERIMENTAL SECTION

2.1. Sample Synthesis and Characterizations. The synthetic route involves a solid-state assembly (SSA) process. Reactions were carried out in sealed silica tubes. The tubes were filled with reaction mixtures under an Ar atmosphere, and then they were evacuated to ~10^{-4} Torr and flame-sealed. In a typical synthesis of CoS_2, Co powder and S powder were used stoichiometrically as raw materials.

Received: May 28, 2012
Accepted: July 25, 2012
Published: July 25, 2012

   dx.doi.org/10.1021/am300951f | ACS Appl. Mater. Interfaces 2012, 4, 4246−4250

The potassium halide (KX; X = Cl, Br, I) serves as the reaction medium and flux agent with the mass ratio of CoS_2/KX = 1:2. The detailed heating procedure is shown in the Supporting Information (Figure S1). After being cooled to room temperature naturally, the powders were collected after washing several times with absolute ethanol and deionized water alternately and dried at 60 °C under vacuum. Phase transformation of cobalt sulfides was investigated by air-annealing CoS_2 in an unsealed silica tube under different temperatures and times.

The crystal structure and phase identification of the samples were obtained by X-ray diffraction (XRD, Bruker D8 ADVANCE) with a monochromatized source of Cu Kα_1 radiation (λ = 0.15405 nm) at 1.6 kW (40 kV, 40 mA). Scanning electron microscopy (SEM, JSM-6510) and field-emission transmission electron microscopy (TEM, JEM 2100F) were employed to study the morphology and particle size of the products.

2.2. Electrochemical Measurements. The as-prepared cobalt sulfides were used as the electrode materials for rechargeable lithium ion batteries. The active materials, acetylene black, and polyvinylidene fluoride (PVDF) were mixed in a weight ratio of 80:10:10 in *N*-methyl-pyrrolidone (NMP) to form a slurry. The working electrodes were fabricated by coating the slurry onto aluminum foils and dried in vacuum at 110 °C for 10 h. The testing coin cells were assembled with the working electrode as-fabricated, metallic lithium foil as a counter electrode, Celgard 2300 film separator, and 1 M $LiPF_6$ in 1:1 ethylene carbonate (EC)/dimethyl carbonate (DMC) as the electrolyte. The assembly of the testing cells was carried out in an argon-filled homemade glovebox (German, M. Braun Co.). The discharge−charge cycle tests were run between 3.0 and 0.5 V using a LAND CT2001A battery test instrument (LAND Electronic Co.). Cyclic voltammetry tests were conducted by a computer-controlled electrochemical workstation (CHI660B, CH Instruments) in the potential range 0.5 to 3.0 V with a scan rate of 0.1 mV s^{-1}.

3. RESULTS AND DISCUSSION

3.1. Solid-State Assembly (SSA) Synthesis of CoS_2. The flux method has been widely used in solid-state synthesis and potassium halides (KX, X = Cl, Br, I) are the common flux agents. In the KX-assisted solid-state reaction, KX promotes the reaction and affects the morphology and size of the final products. Figure 1a shows the X-ray diffraction (XRD) patterns of the samples prepared via the KX-assisted SSA process using different halide fluxes. All peaks of the sample can be assigned to a cubic phase of CoS_2 (JCPDS No.65-3322). Furthermore, the intensity of the diffraction peaks strengthens after using potassium halides.

The corresponding SEM images are shown in Figure 1b, and the obvious difference in morphology and size after adding potassium halides can be observed. When no flux agents were introduced in the reaction system, the CoS_2 shows irregular morphology. While in the presence of KX (X = Cl, Br, I), the products were changed into relatively larger polyhedra, indicating that the KX flux promotes the assembly reaction. Especially in the case of KCl, the size distribution of the final powder is much narrower than those of KBr and KI. It proves that KX plays a vital role in the formation of CoS_2 during the SSA process, which might be due to the varying solubility of CoS_2 in the melt KX. The detailed morphology of the CoS_2 obtained in the KCl-assisted SSA was further characterized by high-magnification SEM and TEM (Figure 2). Figure 2c shows the TEM image of polyhedral CoS_2 after a strongly ultrasonic treatment, indicating that the polyhedron has a plate-like structure. The lattice fringes of CoS_2 can be found clearly in Figure 2d.

3.2. In Situ Transformation of CoS_2. It has been reported that pure CoS is quite difficult to prepare because of the complex stoichiometry of cobalt chalcogenides.[5] In order to synthesize pure CoS, the phase transformation of cobalt sulfides was investigated by annealing CoS_2 at different temperatures in unsealed silica tubes in air. Figure 3a shows the XRD patterns of the samples obtained at 400−800 °C for 10 min. No phase change was observed at 400 °C. As the temperature increased

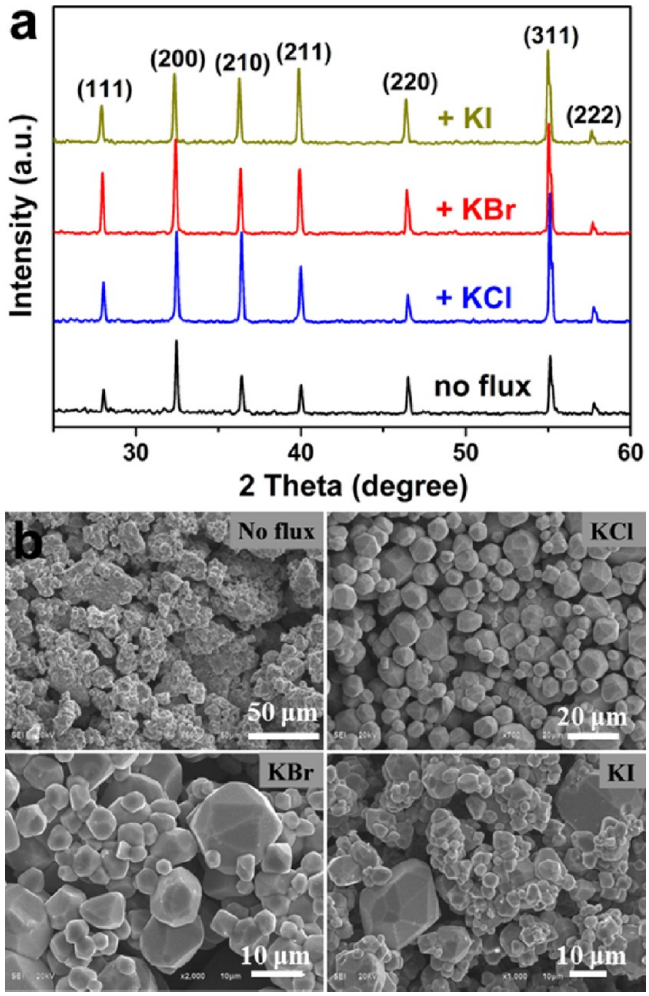

Figure 1. (a) XRD patterns and (b) SEM images of CoS_2 prepared by using different potassium halides.

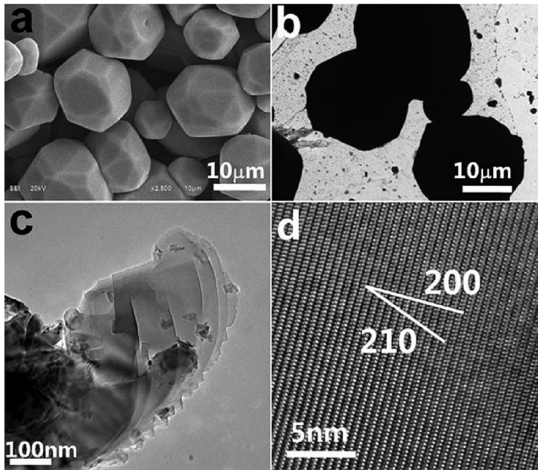

Figure 2. SEM and TEM images of CoS_2 obtained by KCl-assisted SSA process.

dx.doi.org/10.1021/am300951f | ACS Appl. Mater. Interfaces 2012, 4, 4246−4250

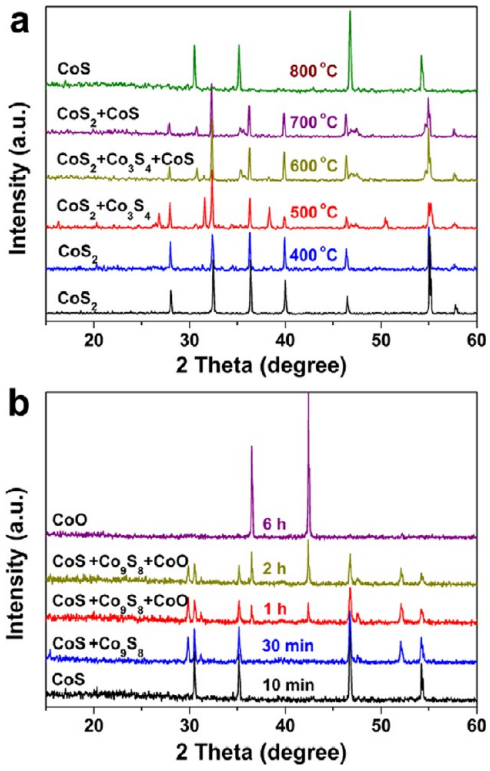

Figure 3. XRD patterns of the samples (a) obtained by in situ transformation of CoS_2 at different temperatures for 10 min and (b) annealed at 800 °C for different times.

to 500 °C, the peaks of Co_3S_4 (JCPDS No. 47-1738) along with CoS_2 were observed. When the temperature further increased to 600−700 °C, the peaks assigned to CoS (JCPDS No. 65-8977 or 3418) were detected. Finally, pure CoS was obtained at 800 °C. The overall morphology keeps almost unchanged only the surface becomes rougher due to the appearance of pores after calcination at 800 °C (Figure 4b).

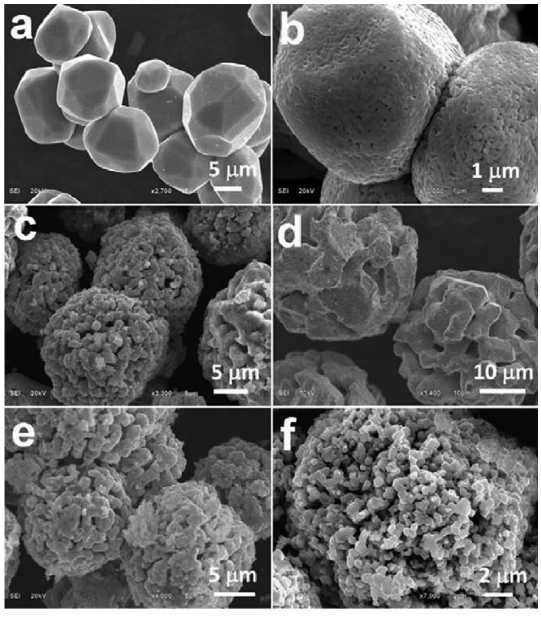

Figure 4. SEM images of cobalt sulfides during the annealing process at 800 °C for different times.

To further investigate the phase transformation of CoS_2 during the calcination in air, the time-dependent experiments were carried out at 800 °C. Figure 3b shows the XRD patterns of the products reacted for 10 min, 30 min, 1 h, 2 h, and 6 h. With the annealing time increased from 10 min to 6 h, the CoS_2 phase transformed to pure CoS, the Co_9S_8 phase (CPDS No. 65-6801), and CoO (CPDS No. 43-1004) in turn. The corresponding SEM images of these samples are shown in Figure 4. Compared with the polyhedral morphology of CoS_2 (Figure 4a), the morphology of CoS remained almost unchanged; only the surface became rougher with the appearance of pores caused by the consumption of sulfur (Figure 4b). After further heating for 30 min, the cobalt sulfides began to calcanei together (Figure 4c). When the annealing time increased to 1 h, the main phases of the sample were still cobalt sulfides, which further aggregated together to form larger particles and pores (Figure 4d) compared with the sample obtained in 30 min. With the time further increased to 2 h, the particle size became smaller due to the oxidation of cobalt sulfides (Figure 4e). Finally, pure CoO with a porous structure was obtained after annealing for 6 h (Figure 4f).

As described above, the evolution of cobalt sulfides involves the consumption of sulfur. From CoS_2 to Co_3S_4 and further to CoS and Co_9S_8, the ratio of S to Co reduced gradually with the increase of annealing temperature or time. When treated at a high temperature of 800 °C for a long time, S was totally consumed and CoO was formed. The in situ transformation of CoS_2 can be described as follows:

$$CoS_2 \xrightarrow{\Delta} CoS_x + (2 - x)S\uparrow \quad (2)$$

$$S + O_2 \xrightarrow{\Delta} SO_2\uparrow \quad (3)$$

$$CoS_x + xO_2 \xrightarrow{\Delta} CoO + xSO_2\uparrow \quad (4)$$

The oxygen in air plays an important role in the evolution of cobalt sulfides, which promotes the consumption of sulfur. In the first stage, CoS_2 was thermally decomposed under calcination and gaseous sulfur was generated according to eq 2. The generated gaseous sulfur would act as protection gas to prevent the direct oxidation of cobalt sulfides. At the same time, the sulfur reacted with the oxygen as shown in eq 3. There exists a balance between the generation and consumption of sulfur. The generated sulfur sufficiently protected the cobalt sulfides in the early stage (<1 h), while with the increasing calcination time, the sulfur was used up and the cobalt sulfides were oxidized (see eq 4). The influence of oxygen in the evolution of cobalt sulfides can be further demonstrated by the following experiment. CoS_2 was sealed in a vacuum silica tube and annealed at 800 °C for 10 min. The phase evolution was hindered, and the phases of CoS_2 and CoS instead of pure CoS were obtained in this case (Supporting Information Figure S2).

It is worth noting that this SSA method can be explored to prepare other cobalt chalcogenides; e.g., $CoSe_2$ and CoSSe are selected for investigation. The corresponding XRD and SEM information is provided in the Supporting Information (Figure S3), presenting the polyhedral morphology and pure phase.

3.3. Properties of Lithium Ion Batteries. As reported, the cobalt sulfides possess a high discharge capacity, whereas the values reduced sharply during the first few cycles in the previous reports.[2,4,5] Thus, it is highly desirable to synthesize cobalt sulfides with better stability. The electrochemical performance of the as-prepared cobalt sulfides (CoS_2 and

CoS) as the electrode materials of lithium ion batteries was evaluated. Figure 5a–b illustrates the charge–discharge curves

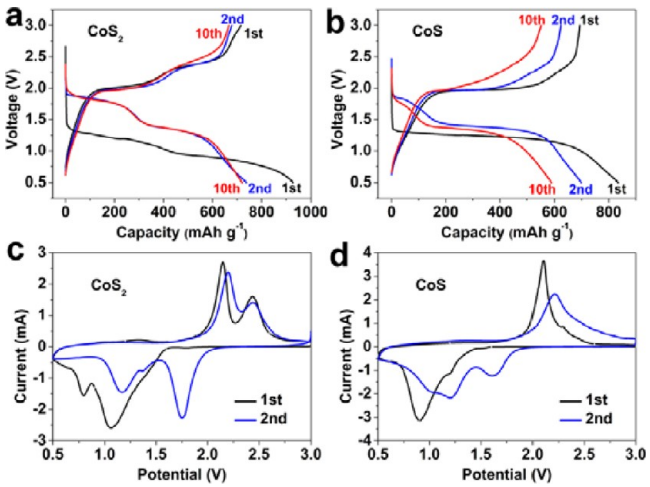

Figure 5. (a, b) Charge–discharge curves of the batteries based on the as-prepared CoS_2 and CoS polyhedrons in the charge/discharge voltage range 0.5–3.0 V; (c,d) Cyclic voltammograms for CoS_2 and CoS polyhedrons with a scan rate of 0.1 mV s^{-1} in the potential range 0.5–3.0 V.

of the samples in the 1st, 2nd, and 10th cycles in the voltage range 0.5–3.0 V at a current density of 100 mA g^{-1}. The first discharge curves are different from the others, consistent with the previously reported results.[2,4] After the first cycle, the two electrodes exhibit similar discharge curves with two voltage plateaus. For both CoS_2 and CoS, the two plateaus in the ranges 1.9–1.5 V and 1.5–1.3 V correspond to the initial insertion of lithium and the following displacement reaction of Li_2S + Co, respectively.[20] In the first charge–discharge cycle, the CoS_2 electrode displays a high discharge capacity of 929.1 mAh g^{-1} and a charge capacity of 716.2 mAh g^{-1}, and the values for the CoS electrode are 835.2 and 693.2 mAh g^{-1} respectively. The irreversible capacity in the first cycle may be attributed to the formation of the solid-electrolyte interphase film on the surface of the electrode materials.[21] Figure 5c–d display the cyclic voltammograms for CoS_2 and CoS polyhedrons with a scan rate of 0.1 mV s^{-1} in the potential range 0.5–3.0 V. For CoS_2, two main reduction peaks at 0.8 and 1.1 V and two oxidation peaks at 2.1 and 2.4 V are observed in the first scanning cycle, while, for CoS, the reduction peaks are located at 0.9 and 1.2 V and the oxidation peaks are located at 2.1 and 2.3 V. Whereas, all the reduction and oxidation peaks have a shift in the subsequent cycle for both CoS_2 and CoS, which is very consistent with the charge–discharge plateaus. The peak areas decrease as the cycle number increases, indicating the reduction in discharge capacity.

Figure 6 displays the cycle and rate performance of CoS_2 and CoS, presenting good cycle performance of the as-prepared samples. The discharge capacities of 720.4 and 589.6 mAh g^{-1} remain after 10 cycles, which is above 76% and 71% of the first discharge capacities for CoS_2 and CoS respectively. Expecially for CoS_2, the discharge capacity was almost unchanged from the 2nd to 10th cycle (738 and 720 mAh g^{-1} respectively). The good reversibility was further demonstrated by the fact that the capacity values 693.7 and 567.2 mAh g^{-1} are retained for CoS_2 and CoS once the rate reverted to 100 mA g^{-1} after rate measurements. The polyhedral cobalt sulfides exhibit a higher

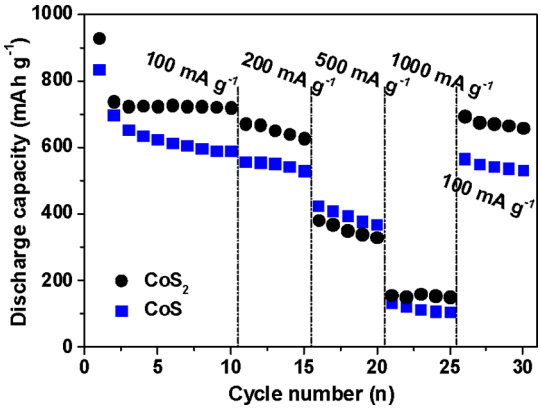

Figure 6. Cycle performance of the batteries based on the as-prepared CoS_2 and CoS polyhedrons.

capacity and better rate performance than the samples prepared by solid methods in previous reports (Table 1), showing promising potential applications in high energy density lithium ion batteries.

Table 1. 10-Cycle Reversible Capacities at a Current Density of 100 mAh g^{-1} in This Work and the Literature

material	capacity (mAh g^{-1})	preparation	source
CoS_2	720	SAA	this work
	530	solvothermal	ref 22
	480	solid reaction	ref 12
	400	solid reaction	ref 23
CoS	589	SAA	this work
	420	solvothermal	ref 24

The above-mentioned cobalt sulfides can transfer to pure CoO with a porous structure after annealing for 6 h in atmosphere. Due to its high theoretical Li ion storage capacities (716 mAh g^{-1}) and its completely reversible electrochemical reaction,[25] the lithium storage performance of the porous CoO is also studied here. As shown in Figure 7a, the initial discharge capacity of CoO is 470 mAh g^{-1}. Two discharge platforms at voltage potentials of 1.1 and 0.7 V are observed in the first discharge curve, while they disappeared in the second discharge curve, which is due to the irreversible formation of a solid electrolyte interphase (SEI) and the decomposition of electrolyte.[26] In the second cycle, the discharge platform shifted to 1.4 V. Compared with CoO, the CoO/cobalt sulfides composite shows a higher discharge platform at 1.3 V and a higher initial discharge capacity of 521 mAh g^{-1}. The enhanced capacity may be due to the existence of cobalt sulfides, which has good conductivity and high capacity.

The rate performance of CoO and the CoO/cobalt sulfides composite is shown in Figure 7b. The sample with cobalt sulfides existing exhibits better rate performance than pure CoO. The capacity of the CoO/cobalt sulfides composite decreases steeply from 368 mAh g^{-1} (after 20 cycles) to 231 mAh g^{-1} with an increasing current rate from 100 mAh g^{-1} to 500 mAh g^{-1}, and the capacity loss is 37.2%. For CoO, the capacity decreases from 306 to 70 mA h g^{-1}, and the capacity loss is 77.1%. This result further demonstrates that highly conductive cobalt sulfides can significantly improve the rate performance of pure CoO.

dx.doi.org/10.1021/am300951f | ACS Appl. Mater. Interfaces 2012, 4, 4246–4250

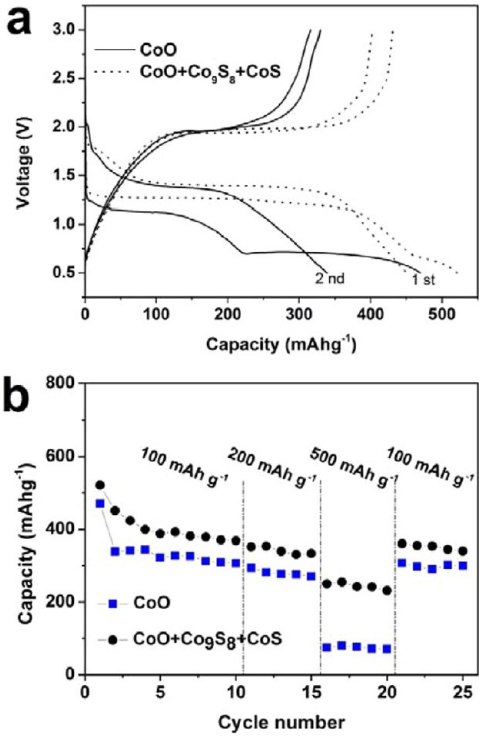

Figure 7. (a) Charge−discharge curves of CoO and CoO/cobalt sulfides composite; (b) rate performance of the batteries based on the CoO and CoO/cobalt sulfides composite.

CONCLUSION

In summary, CoS_2 polyhedra were prepared by a facile potassium halide (KX; X = Cl, Br, I) assisted solid-state assembly (SSA) reaction. The flux of KX played a crucial role in the formation process and the size distribution of the final products, and KCl was optimal. The cobalt sulfide of CoS was easily obtained by annealing CoS_2 in an unsealed silica tube in air at 800 °C for 10 min. Furthermore, this facile KX-assisted SSA method was used to prepare $CoSe_2$ and CoSSe. The as-prepared cobalt sulfides were successfully applied as the electrode materials in lithium ion batteries. The discharge capacities of 929.1 and 835.2 mAh g^{-1} were gained in the voltage range 3.0 to 0.5 V for CoS_2 and CoS, and above 76% and 71% of the capacities can be retained after 10 cycles. High capacities and good cycle performance of the as-prepared cobalt sulfides make them promising candidates for rechargeable lithium ion batteries. The proposed KX-assisted SSA is a powerful and cost-effective approach to the mass production of metal chalcogenides.

ASSOCIATED CONTENT

Supporting Information

The heating procedure of the solid-state assembly (SSA) process, XRD and SEM analysis. This material is available free of charge via the Internet at http://pubs.acs.org.

AUTHOR INFORMATION

Corresponding Author

*E-mail: huangfq@mail.sic.ac.cn; xzhang@mail.neu.edu.cn. Fax: +86 21 5241 6360.

Notes

The authors declare no competing financial interest.

ACKNOWLEDGMENTS

This work was financially supported by National 973 and 863 Program of China Grant Nos. 2009CB939903 and 2011AA050505; National Science and Technology Major Project Grant No. 2011ZX02707; NSF of China Grant Nos. 21101164, 20901083, 91122034, 50821004, 51125006, and 51102263; NSF of Shanghai Grant No.11ZR1441900; and Science and Technology Commission of Shanghai Grant Nos. 10520706700 and 10JC1415800. The authors thank Prof. I-Wei Chen at the University of Pennsylvania for the insightful suggestions.

REFERENCES

(1) Hoodless, R. C.; Moyes, R. B.; Wells, P. B. *Catalysis Today* **2006**, *114*, 377−382.
(2) Yan, J.; Huang, H.; Zhang, J.; Liu, Z.; Yang, Y. *J. Power Sources* **2005**, *146*, 264−269.
(3) Wang, J.; Ng, S. H.; Wang, G. X.; Chen, J.; Zhao, L.; Chen, Y.; Liu, H. K. *J. Power Sources* **2006**, *159*, 287−290.
(4) Wang, Q.; Jiao, L.; Han, Y.; Du, H.; Peng, W.; Huan, Q.; Song, D.; Si, Y; Wang, Y.; Yuan, H. *J. Phys. Chem. C* **2011**, *115*, 8300−8304.
(5) Wang, Q.; Jiao, L.; Du, H.; Peng, W.; Han, Y.; Song, D.; Si, Y; Wang, Y.; Yuan, H. *J. Mater. Chem.* **2010**, *21*, 327−329.
(6) Song, D.; Wang, Y.; Han, Y.; Li, L.; Liu, G.; Jiao, L.; Yuan, H. *J. Power Sources* **2010**, *195*, 7462−7465.
(7) Malwah, M.; Bene, R.; Walser, R. *J. Appl. Phys.* **1975**, *46*, 2250−2256.
(8) Otero-Leal, M.; Rivadulla, F.; Rivas, J. *Magnetics, IEEE Transactions on* **2008**, *44*, 4503−4505.
(9) Pasquariello, D.; Kershaw, R.; Passaretti, J.; Dwight, K.; Wold, A. *Inorg. Chem.* **1984**, *23*, 872−874.
(10) Winter, M.; Brodd, R. J. *Chem. Rev.* **2004**, *104*, 4245−4270.
(11) Apostolova, R.; Shembel', E.; Talyosef, I.; Grinblat, J.; Markovsky, B.; Aurbach, D. *Russ. J. Electrochem.* **2009**, *45*, 311−319.
(12) Luo, W.; Xie, Y.; Wu, C.; Zheng, F. *Nanotechnology* **2008**, *19*, 075602.
(13) Poizot, P.; Laruelle, S.; Grugeon, S.; Tarascon, J. M. *J. Electrochem. Soc.* **2002**, *149*, A1212−A1217.
(14) Débart, A.; Dupont, L.; Patrice, R.; Tarascon, J. M. *Solid State Sci.* **2006**, *8*, 640−651.
(15) Gao, J.; Li, Q.; Zhao, H.; Li, L.; Liu, C.; Gong, Q.; Qi, L. *Chem. Mater.* **2008**, *20*, 6263−6269.
(16) Si, P. Z.; Zhang, M.; Zhang, Z. D.; Zhao, X. G.; Ma, X. L.; Geng, D. Y. *J. Mater. Sci.* **2005**, *40*, 4287−4291.
(17) Remskar, M.; Mrzel, A.; Skraba, Z.; Jesih, A.; Ceh, M.; Demšar, J.; Stadelmann, P.; Lévy, F.; Mihailovic, D. *Science* **2001**, *292*, 479−481.
(18) Du, G.; Li, W.; Liu, Y. *J. Phys. Chem. C* **2008**, *112*, 1890−1895.
(19) Chang, K.; Chen, W. *Chem. Commun.* **2011**, *47*, 4252−4254.
(20) Kim, Y.; Goodenough, J. B. *J. Phys. Chem. C* **2008**, *112*, 15060−15064.
(21) Wu, M. S.; Chiang, P. C. J. *Electrochem. Commun.* **2006**, *8*, 383−388.
(22) Wang, Q.; Jiao.; Han, Y. *J. Phys. Chem. C* **2011**, *115*, 8300−8304.
(23) Yan, J. M.; Huang, H. Z.; Zhang, J.; Liu, Z. J.; Yang, Y. *J. Power Sources* **2005**, *146*, 264−269.
(24) Wang, Q.; Jiao, L.; Du, H.; Peng, W.; Han, Y.; Song, D.; Si, Y.; Wang, Y.; Yuan, H. *J. Mater. Chem.* **2011**, *21*, 327−329.
(25) Aricò, A. S.; Bruce, P.; Scrosati, B.; Tarascon, J. M.; Schalkwijk, W. V. *Nat. Mater.* **2005**, *4*, 366−377.
(26) Nam, K. T.; Kim, D. W.; Yoo, P. J.; Chiang, C. Y.; Meethong, N.; Hammond, P. T.; Chiang, Y. M.; Belcher, A. M. *Science* **2006**, *312*, 885−888.